International Review of Electrical Engineering (I.R.E.E.), Vol. 9, N. 4
ISSN 1827- 6660 pp.873-881 July – August 2014

Power Arcing Source Location Using First Peak Arrival of RF-Signal

Frank Zoko Ble, Matti Lehtonen, Ari Sihvola, Charles Kim

Abstract – *This paper reports an experimental investigation of locating arc sources using strategically placed antennas and the signal arrival times of first peak component of the wide-band electromagnetic signals radiated from the sources toward the antennas. Theoretical approaches of such electromagnetic source location are first introduced and then a new approach of using the dominant frequency component of the first peak wave to clarify the source location distance is discussed. Experiments of arc generation and radiation signal measurement are conducted and, using the measured electromagnetic data, the arc source location method is applied and the results are compared against the actual location. It is found that the first peak arrival method works at a reasonable level of accuracy.*

Keywords: *Power Arc, Radio Frequency, Electromagnetic Radiation, Antenna, Signal Arrival Time, Arc Source Location, Signal Processing, Radio Signal Propagation, Time Delay Estimation, Radio Measurement*

Nomenclature

FD	Directional Finding
PA	Propagation Attenuation
RF	Radio Frequency
TDOA	Time Difference of Arrival
DDOA	Distance Difference of Arrival
DOA	Distance of Arrival
TOA	Time of Arrival
ASCC	Arc Source Cartesian Coordinates
ant_1	Antenna 1
LSM	Least Square Method
D_{ij}	Distance delay
d_{ij}	Distance difference of arrival
t_{ij}	Signal time difference of arrival
$n_x(t)$	Wide-sense Gaussian noise
c	Speed of signal wave (speed of light)
$s(t)$	RF-Signal
τ	Time delay
$F(X)$	Non-linear vector function
$X(x_i, y_i, z_i)$	Vector variable
DMS	Distribution Management System
OMS	Outage Management System
FPA	First Peak of Arrival

I. Introduction

This paper investigates fault location based on radio signals produced by arcing faults in power systems. In distribution overhead line networks, numerous problems can result in arcing faults.

These problems include trees coming into contact with power lines, dirty insulators, as well as various other types of insulation failures. [1] The difficulty in dealing with such power arcs is that this type of fault induces low currents that are undetectable by existing conventional methods such as circuit breakers and relays, thus placing the entire system at risk [2]. Therefore, location of arcing faults is valuable for utility that operates and maintains a distribution system. Some attempts in [1]-[7] have been made to locate power arc by utilizing the radio frequency (RF) signals generated from the arc.

This paper aims to add knowledge to this new area of arc location via Radio Frequency (RF) signal. It is hoped that a good detection system for arc-induced electromagnetic wave using multiple strategically placed antennas could soon be integrated to the distribution management system (DMS) and/or outage Management system (OMS) for accurate location of fault arcs and faster power supply restoration and minimized outage hours. Due to a large geographical area of distribution system, the identification antennas must be placed perhaps in the area where power arcs are frequently reported by the maintenance technicians. These antennas can be mounted on the poles under the overhead lines.

When an arc fault occurs, the associated time-varying currents create electromagnetic radiation into the surrounding space like a transmitting antenna. The spectrum of the radiation is very wide due to the strong irregularity of the time variation of the power arc. The radiated wave is carried by electric and magnetic fields which couple to each other according to Maxwell's differential equations. Even if the time dependence of the radiated wave is not monochromatic, each of a sinusoidal component travels with the speed of light to all directions

away from the arc. The amplitude of the radiated signal attenuates with increasing distance not only due to the fact that the power density of a spherical wave decreases but also due to absorption and scattering of the electromagnetic energy by the structures and inhomogeneity in the environment.

This electromagnetic wave can be recorded and the time of arrival information gathered by the distributed receiving antennas, enabling the position of the arcing fault to be located [1]-[7], [10]-[13]. This paper discusses in section II the existing radio location methods followed by the arc location experiments in section III in which description of the experiments and measurement data are discussed. Subsequently, source location using measured data via radio energy level and radio wave first peak arrival is described. Then, the description of the spectrum peak arrival time, and its application for source finding for a complete fault location algorithm is presented.

Also, overall source location results are discussed. Finally, in section IV, the conclusions are presented with suggested improvements.

II. Power Arc Detection and Location Methods

There are several approaches of RF-signal based electromagnetic radiation source location. One method relies on multiple directional antennas placed around a possible source to decide the location [2], [3], [7], [9], [14], [15]. The intersection of the concentric magnitude pattern or the highest peak point made out from the magnitude contour pattern of the antennas would produce the source.

Another group of methods estimates time delays of electromagnetic signal arrival time at different antennas placed in different distance, and finds distance to the source using the time differences. [1]-[16] Similar but slightly different methods utilize the propagation times, not the difference in arrival times (TDOA), registered at the antennas located in different places and then estimate the source location. [17], [13]-[23]

Below is a brief description of the common features of the above mentioned RF-signal arrival-time based methods. The basic aspect of the common features is that, by the placement of the antennas, they determine a RF signal source using the moments or time differences the RF-signal arrived at different antennas. Under this concept, with an antenna *i* located at (x_i , y_i , z_i), for example, and the source location coordinate (x_s , y_s , z_s).

The equation for the distance between the source and the antenna can be expressed by RF signal arrival time at antenna *i*, t_i multiplied by the speed of the RF signal *c* as follows:

$$t_i \cdot c = \sqrt{(x_s - x_i)^2 + (y_s - y_i)^2 + (z_s - z_i)^2} \qquad (1)$$

Similar relationship to the above can be obtained from antennas for $i = 2 \ldots n$, where n is the total number of antennas placed. Using the above relationship in (1), an accurate estimate of the arcing source coordinate is determined from the measured times of arrival (TOA) and the coordinates of the antennas. [1]

In order to estimate the time delay or TOA, two antennas are needed to capture the transmitted signal $s(t)$. Assuming that the signal $y(t)$ received at antenna ant_2 is the replica of $x(t)$ captured by antenna ant_1 but being delayed by time t_{12}. The signals $x(t)$ and $y(t)$ received by a pair of antennas separated by distance $d_{12} \times t_{12}$, are expressed as [1]:

$$\begin{aligned} x(t) &= s(t) + n_x(t) \\ y(t) &= \alpha s(t+\tau) + n_y(t) \end{aligned} \qquad (2)$$

where α is the signal amplitude attenuation factor, $n_x(t)$ and $n_y(t)$ are the wide-sense Gaussian noise processes which are uncorrelated with the signal of interest $s(t)$ and τ is the time delay between the signal arrival time.

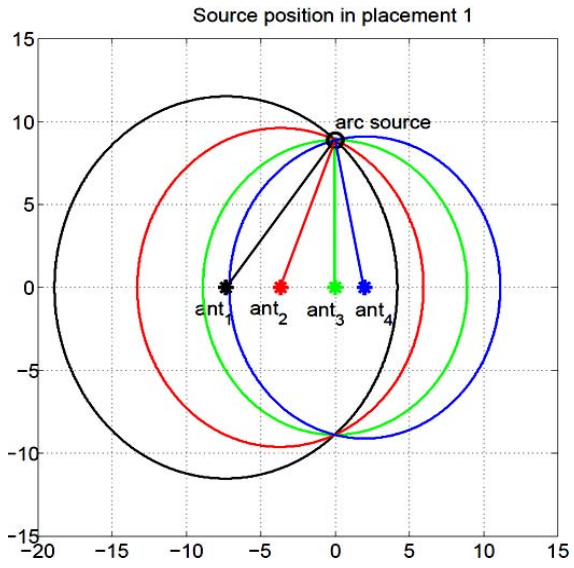

Fig. 1. The source position placed at the intersection of the circles. The measured distances of arrival (DOA) are the radii of the circle centered at each antenna

Another way of locating a source using the same arrival time scheme is to draw a circle of radius corresponding the arrival distance for each antenna as illustrated in Fig. 1. This way is useful especially when omnidirectional antennas are used. The arc source is determined as the intersection point of the distance of arrival (DOA) radii [1]. The time difference of signal arrival (TDOA) at antennas has been popularly adopted for high accuracy in location of a source since the advent of radar.

However, the common problem of the above mentioned arrival time based methods is that, due to the noisy RF signals measured at antenna, the exact arrival time point is not always straightforward.

To solve the problem, we propose a method of arrival time approach for arc source location by using the first arriving peak (FAP) components of the noisy RF signals as to decide the arrival time. An antenna with the peak at the earliest is the closest to the source while the one with peak at the latest, the farthest.

An experimental method of obtaining the needed arrival times (TOA) or the time difference of arrival (TDOA) and the feasibility study of the method proposed using the acquired arrival times are the main subject of the next section.

III. Arc Location Experiment and Data Analysis

In order to evaluate the performance of the proposed method, we performed a set of arc location experiments as shown in Fig. 2 and Fig. 4. As shown in Fig. 4, 5 types of antenna placements were made. These will help to choose the suitable antenna arrangement that could be adopted for power arc fault detection in power distribution network [1].

III.1. Experiment Set-up

The set-up depicted in Fig. 2 consists of four antennas placed around the arc source covering a portion of RF radiation space. The distances between two neighboring antennas vary in interval of 2 to 12 m.

The antennas used as shown in Fig. 3 are Yagi – Uda antennas which cover a frequency range of 47 - 862 MHz with 75 Ω impedance. The Yagi – Uda antenna is commonly known as a Yagi antenna that is a directional antenna consisting of a driven element namely a dipole or folded dipole and additional parasitic elements such as reflector and directors.

The reflector element is slightly longer typically at about 5% than the driven dipole, whereas the so-called directors are a little shorter. Yagi-Uda antennas are directional along the axis perpendicular to the dipole in the plane of the elements, from the reflector toward the driven element and the directors.

Highly directional antennas such as the Yagi-Uda are commonly referred to as beam antennas due to their high gain. However, the Yagi-Uda design only achieves this high gain over a rather narrow bandwidth, making it useful for specific analytical communications bands like high frequency (HF), very high frequency (VHF), and ultra-high frequency (UHF) bands; therefore it is appropriate to be used in the measurements of the experiment. The arc is produced by a pine tree leaning on an iron rod at a gap length of 5 mm, which is located at (0.07, 8.89, 5.1) coordinate measured in meter in the Euclidian plan, away from the closest antenna (used as a reference antenna) which takes turns among the antennas according to placement variations: antenna 3 in placement 1, antenna 4 in placement 2, antenna 4 in placement 3, antenna 2 in placement 4 and antenna 1 in placement 5.

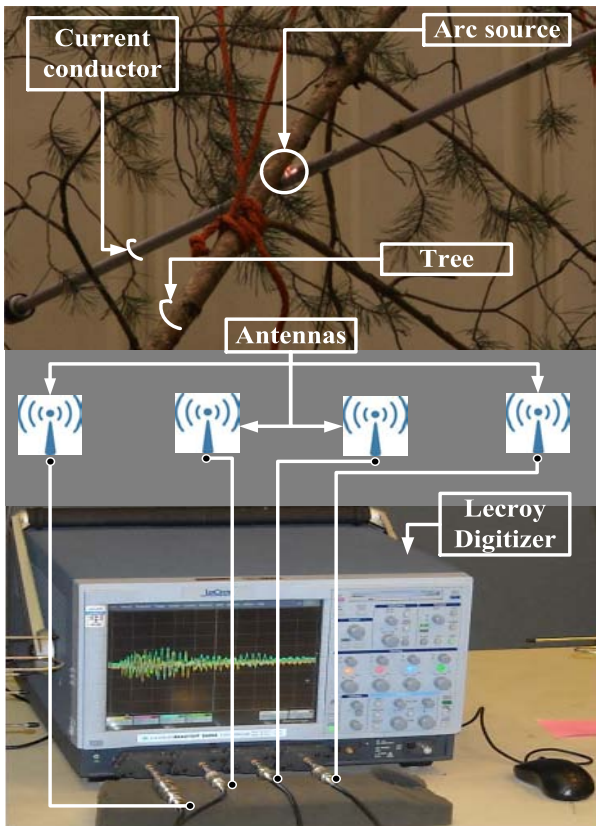

Fig. 2. The experimental setup for arc generation. A high voltage AC source of 20 kV is used to generate the arcs. The arc is produced by tree leaning on an iron rod

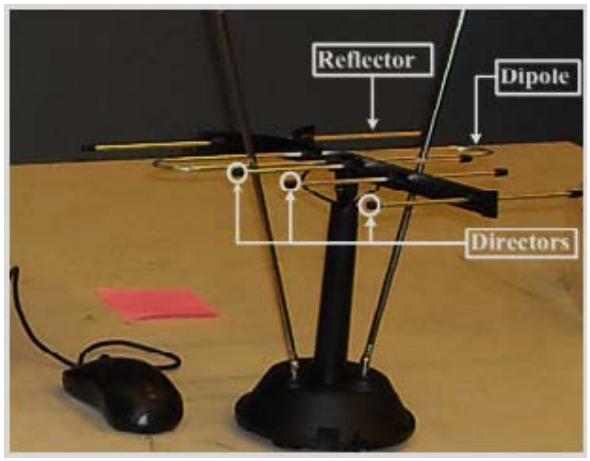

Fig. 3. The Yagi-Uda array which covers a frequency range of 47 - 862 GHz

A high voltage AC source (voltage generator 0 ~ 260 V) feeding a transformer of 20/0.4 kV is used to generate the arcs. Fig. 2 shows the actual arc produced between the conductor and a pine tree during the experiment carried out in the high voltage laboratory at Aalto University of Finland.

The output of each antenna is connected through coaxial cable of 3 m to a multi-channel LeCroy digitizer of 2 GHz/s sampling frequency in order to capture the radiated RF signals from the arcs. The pine tree roots are placed in a bowl filled with water in order to maintain the tree in its natural environment conditions. The tree's total length is 9 m and it was leaning on the metallic rod at about 5.1 m from the floor. The tree has a diameter of 75 mm at its bottom and 58 mm at the point where the arc is produced. The arc current and voltage across the tree is measured and recorded. Having obtained the current and voltage values, the tree's resistance is determined at about 316 kΩ. For each channel, signals are captured at the sample rate of 20000 samples per microsecond as illustrated in Fig. 5.

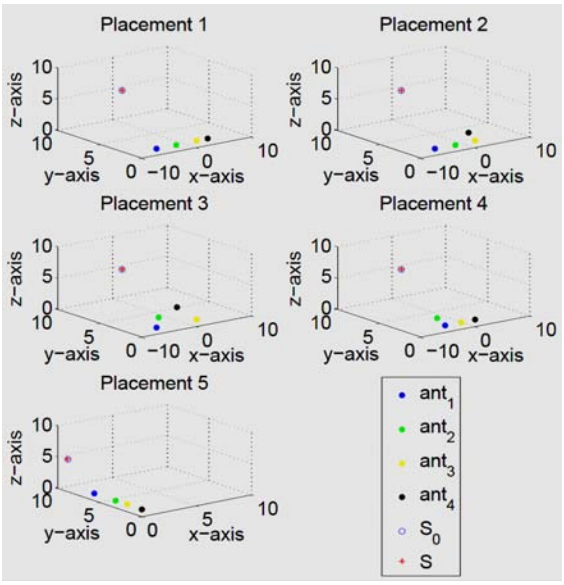

Fig. 4. Antenna placements [1]

As shown in Figure 4 the five placement methodologies are done as follow:

a. Placement 1: the antennas are horizontally placed on the *x*-axis with ant 1 (-7.35, 0, 1.1), ant 2 (-3.68, 0, 1.1), ant 3 (0, 0, 1.1), and ant 4 (2, 0, 1.1).
b. Placement 2: antennas 1, 2 and 3 are horizontally placed on *x*-axis and the antenna 4 is slightly shifted toward to the arc source, with ant 1 (-7.35 , 0 , 1.1), ant 2 (-3.68 , 0 , 1.1), ant 3 (0 , 0 , 1.1), and ant 4 (2 , 2.1 , 1.1).
c. Placement 3: the antennas 1 and 3 remain on the on *x*-axis while antennas 2 and 4 are placed much closer to the arc source with ant 1 (-7.35, 0, 1.1), ant 2 (-3.68 , 2.1 , 1.1), ant 3 (0 , 0 , 1.1), and ant 4 (2 , 3.63 , 1.1).
d. Placement 4: the antennas 1, 3 and 4 are horizontally placed on *x*-axis and the antenna 2 is moved forward and closer to the arc source point with ant 1 (-5.53 , 0 , 1.1), ant 2 (-3.76 , 2.1 , 1.1), ant 3 (-2.60 , 0 , 1.1), and ant 4 (0 , 0 , 1.1).
e. Placement 5: The 4 antennas are all vertically placed on *y*-axis with ant 1 (0 , 5.71 , 1.1), ant 2 (0 , 3.16 , 1.1), ant 3 (0 , 1.74 , 1.1), and ant 4 (0 , 0 , 1.1).

In the legend of Fig. 4 ant_i (with i = 1, 2, 3, 4) stands for antenna. S_o and S are respectively the actual and measured source points. From the arrangement of the antennas, the theoretical arrival times of the radiated signal first peak amplitude sent by the arc are calculated and the results are presented in Table I.

In order to avoid the signal corruption due to the surrounding free space interferences, only the first arrival peak of the signal is considered. The measurement room size is 21 m × 15 m × 15 m, and the antennas are placed at about 10 m from the wall surface and 12 m from the ceiling thus the signal reflections are avoided for the FPA of signals integrity.

TABLE I
ACTUAL TIME OF ARRIVAL TOA [ns]

Placement	t_1	t_2	t_3	t_4
1	40.716	34.745	32.495	33.165
2	40.712	34.742	32.495	27.095
3	40.710	29.002	32.495	23.007
4	37.371	29.116	33.637	32.495
5	17.033	23.293	27.309	32.495

TABLE II
ACTUAL TIME DIFFERENCE OF ARRIVAL BETWEEN THE ANTENNAS (TDOA) [NS]

Placement	t_{12}	t_{13}	t_{14}	t_{23}	t_{24}	t_{34}
1	5.963	8.201	7.524	2.238	1.561	0.677
2	5.963	8.201	13.594	2.238	7.632	5.393
3	11.704	8.201	17.682	3.503	5.978	9.481
4	8.254	3.728	4.864	4.525	3.389	1.136
5	6.260	10.276	15.461	4.016	9.201	5.185

TABLE III
ACTUAL DISTANCE OF ARRIVAL (DOA) [m]

Placement	d_1	d_2	d_3	d_4
1	12.215	10.424	9.748	9.949
2	12.214	10.423	9.748	8.128
3	12.213	8.700	9.748	6.902
4	11.211	8.735	10.09	9.748
5	5.110	6.988	8.193	9.748

TABLE IV
ACTUAL DISTANCE DIFFERENCE OF ARRIVAL (DDOA) [M]

Placement	d_{12}	d_{13}	d_{14}	d_{23}	d_{24}	d_{34}
1	1.791	2.467	2.266	0.675	0.474	0.201
2	1.791	2.465	4.085	0.674	2.294	1.620
3	3.513	2.465	5.311	1.048	1.798	2.846
4	2.477	1.120	1.463	1.356	1.014	0.343
5	1.878	3.083	4.638	1.205	2.760	1.556

From the assumption that the arc RF signals travel at the speed of light, the theoretical RF signal arrival times (TOA) per placement are calculated using (1), from t = 0 of arc onset, in antenna j from arc source with (j = 1, 2, 3, 4), t_{0j} for each of the four antennas in placement 1 is as follows: t_{01} = 40.716 ns, t_{02} = 34.745 ns, t_{03} = 32.495 ns and t_{04} = 33.165 ns. Similarly the other theoretical TOA in each placement are calculated and presented in Table I. The distance from the source to each of the antennas by the time arrival is calculated and presented in Table III.

The signal times differences of arrival (TDOA) between pairs of antennas are then derived by taking the algebraic subtraction between pair of TOA and the results are illustrated in Table II.

From the results obtained in Table II, the actual distance differences between pairs of antennas are also calculated and presented in Table IV.

The explanation of the calculation results in the tables discussed above is done in detail in the next section.

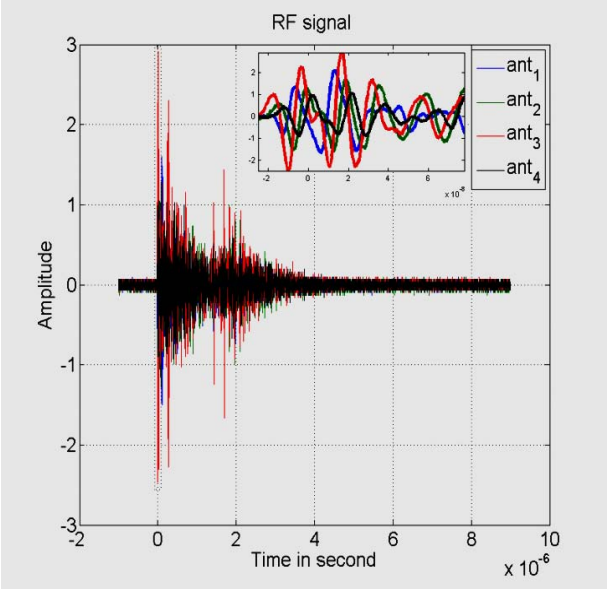

Fig. 5. The captured arc RF signal in placement 1

The gathered data by the digitizer snapshot of the time expanded waveform in the receivers' channels is plotted using Matlab as illustrated in Figure 5 for placement 1, in which antenna 3 is close to the arc source point which presents much higher FPA amplitude compared to the others as expected. From these 5 different placements, the signal time and distance difference of arrival are then calculated and the entire results are presented respectively in Tables VI and VII.

The algorithm used to derive the exact arc source point location based on the captured signal data is explained in detail in the next paragraph.

III.2. Measured Data Analysis Algorithm

The first peak detection finds the crests with the highest amplitude in the received waveforms and uses the difference to calculate the TDOA as is illustrated in Fig. 6. To do so, pair of signal is considered.

For instance using two signals namely antenna 1 (ant_1) and antenna 2 (ant_2), the first peak times of arrival as shown in Table V are calculated by dividing the first peak corresponding sample number (N_i) by the total number of samples (N). As seen in Fig. 6, N_1 and N_2 are respectively the first peak sample number of antenna 1 and antenna 2. A ratio of N_i/N (with N = 20000 and i = 1, 2, 3 and 4) is multiply by the sampling time T_s = 1 ns and thus gives the TOA.

From $[(N_i - N_j)/N] \times T_s$ the TDOA is also determined. The entire results of TOA and TDOA are illustrated respectively in Tables V and VII. Having calculated TOA and TDOA, the distances of arrival DOA and the difference distances of arrival DDOA are directly derived as DOA = c×TOA and DDOA = c×TDOA where c is the speed of signal propagation (similar to the speed of light).

The outcomes of DOA and DDOA are respectively shown in Tables VII and VIII.

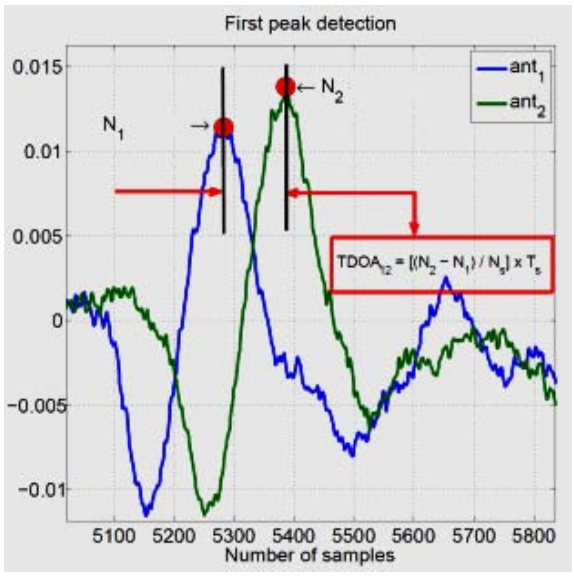

Fig. 6. RF signal first peak time of arrival calculation

TABLE V
MEASERED TIME OF ARRIVAL TOA [Ns]

Placement	t_1	t_2	t_3	t_4
1	33.426	32.78	32.32	32.312
2	35.492	31.035	31.644	32.148
3	34.16	31.76	32.012	31.201
4	33.09	31.219	31.602	31.383
5	24.518	24.966	25.329	25.907

TABLE VI
MEASURED TIME DIFFERENCE OF ARRIVAL BETWEEN THE ANTENNAS (TDOA) [ns]

Placement	t_{12}	t_{13}	t_{14}	t_{23}	t_{24}	t_{34}
1	0.997	1.15	1.198	0.622	0.635	0.334
2	4.51	3.848	3.345	1.584	2.021	0.573
3	2.523	2.159	2.991	1.221	1.115	1.008
4	1.871	1.519	1.707	0.765	0.488	0.363
5	0.497	0.819	1.39	0.364	0.942	0.578

TABLE VII
MEASURED DISTANCE OF ARRIVAL (DOA) [m]

Placement	d_1	d_2	d_3	d_4
1	10.028	9.834	9.696	9.694
2	10.648	9.311	9.493	9.644
3	10.248	9.528	9.604	9.36
4	9.927	9.366	9.481	9.415
5	7.355	7.49	7.599	7.772

TABLE VIII
MEASURED DISTANCE DIFFERENCE OF ARRIVAL (DDOA)[m]

Placement	d_{12}	d_{13}	d_{14}	d_{23}	d_{24}	d_{34}
1	0,299	0,345	0,359	0,187	0,191	0,1
2	1,353	1,154	1,003	0,475	0,606	0,172
3	0,757	0,648	0,897	0,366	0,335	0,302
4	0,561	0,456	0,512	0,23	0,146	0,109
5	0,149	0,246	0,417	0,109	0,283	0,173

III.3. Results and Discussion

According to [1] the solution of (1) is formed by an application of the Newton–Raphson technique to solve the nonlinear function illustrated in (3). The equation (3) is a reformulation of (1) and yields a nonlinear function vector F(X) to be solved with numerical methods, like least square method (LSM):

$$F(X) = \sqrt{(x_s - x_i)^2 + (y_s - y_i)^2 + (z_s - z_i)^2} - D_{ij} \quad (3)$$

$F(\mathrm{X})$ is a non-linear vector function discussed in detail in [1] and $X = (x, y, z)$ is a vector variable.

Function $F(\mathrm{X})$ is expanded using Taylor's series in vicinity of the root iteration $\mathrm{X}^0 = (x^0, y^0, z^0)$ as the iteration guess point. Table IX presents the iteration outcomes results.

The guess point was set at (0.07, 8.8, 5) and the non-linear system (3) was solved after 5 iterations when the sum of squared function values reaches 1.58e-025 that is less than square root of the function tolerance default set as 1.e-003. With the relative norm of the gradient of the sum of squared function values of 9.41e-015, and that is less than the product of 1e-4 by the square root of the function tolerance which rapidly converges close to 1.e-010, thus completed the iteration when the vector of function values also converge near zero as illustrated in Table IX. Finally Table X shows the entire result of the arc source *x*-*y*-*z* coordinates (ASCC).

From the observation of Table X, the *x*-coordinates of the calculated arc source point in these 5 placements are shifted from the actual source value by 0.3462, 0.2010, 0.0837, 0.2440 and 0.1250 m respectively for placements 1, 2, 3, 4 and 5.

The *y*-coordinates are shifted in the same order by 0.4167, 0.2271, 0.0856, 0.2095 and 0.0610 m**.** Similarly *z*-coordinates are displaced by 0, 0.3689, 0.1536, 0.3404 and 0.1371 m and the error summary between the actual and the measured source Cartesian coordinates (ASCC) are shown in Table XI.

TABLE IX
ITERATION RESULTS

Iteration	Func-count	Residual	1rst order optimality	Lambda	Norm of step
0	4	1145.02	602	0.01	
1	8	148168	44.3	0.001	1.74278
2	12	0.0013239	0.518	0.0001	0.190718
3	16	3.01e-011	7.82e-005	1e-05	0.002340
4	20	1.58e-025	5.66e-012	1e-06	3.53e-007

TABLE X
ARC SOURCE POSITION

Placement	Actual source			Measured source		
	x	*y*	*z*	*x*	*y*	*z*
1	0.0696	8.8771	5.0942	-0.1326	8.1057	5.0942
2	0.0696	8.8771	5.0942	-0.0478	8.4566	4.8927
3	0.0696	8.8771	5.0942	0.1185	9.0356	5.1781
4	0.0696	8.8771	5.0942	-0.0729	8.4892	4.9083
5	0.0696	8.8771	5.0942	0.0715	8.7641	5.0193

TABLE XI
ERROR IN ASCC [m]

Placement	*x*	*y*	*z*
1	0.2022	0.7714	0.0000
2	0.1174	0.4205	0.2015
3	0.0489	0.1585	0.0839
4	0.1425	0.3879	0.1859
5	0.0730	0.1130	0.0749

The calculated ASCC are scattered as presented in Figs. 7, 8, 9 and 10 with colored dot (□) marks, along with the true coordinate of the arc source which is marked by red filled small circle in Fig. 8 and by blue filled circle (○) in Figs. 7, 9 and 10.

From Figures 7, 9 and 10 one can clearly observe that the measured arc source point per placement lies inside the unit circle centered at the true source. This implies that the method of the first peak arrival of signal components shows certain accuracy and is scientifically meaningful.

Similar observation can be seen in Figure 8 where the measured arc sources per placement are all within a unit sphere with its center gravity at the actual source point.
The performance of this first arrival peak method is quite promising as the measured source points are displaced from the actual source with maximum error at about 0.4167 in per unit scale taken from the data illustrated in Table X. The measured source is displaced from the actual position with an accuracy of 0.7975, 0.4459, 0.1676, 0.4209 and 0.1361 m respectively for the placements 1, 2, 3, 4 and 5.

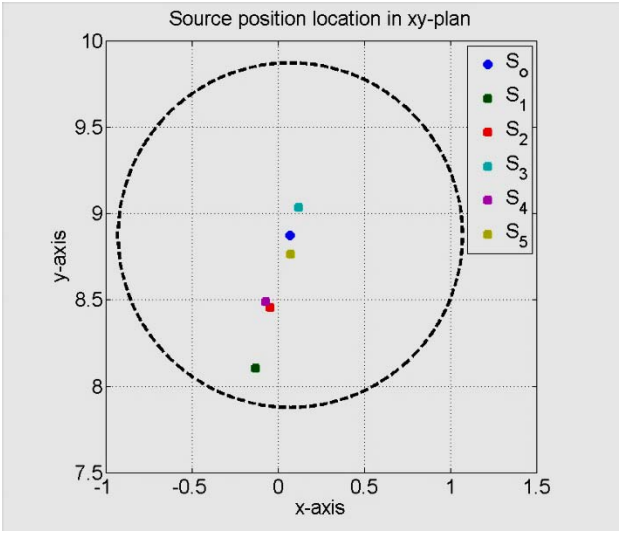

Fig. 7. Measured and actual sources observed in 2D (x , z)-plan

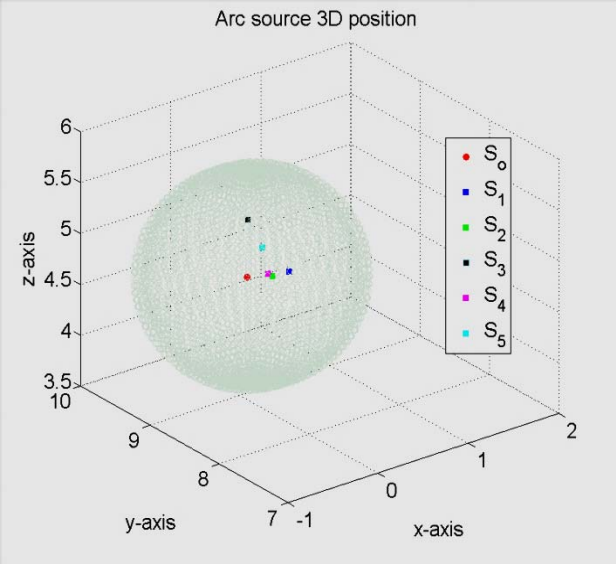

Fig. 8. Measured and actual sources observed in 3D Cartesian plane

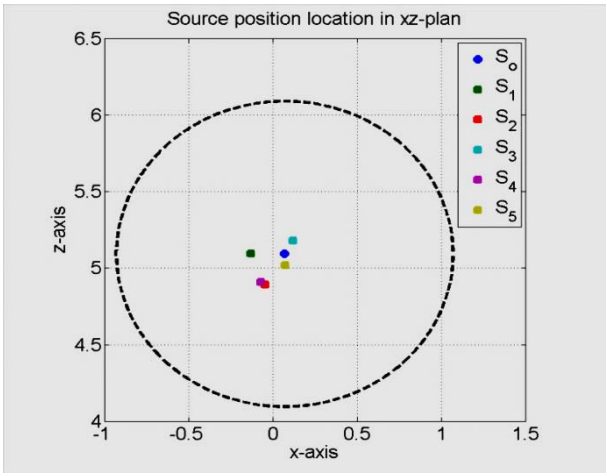

Fig. 9. Measured and actual sources observed in 2D (x , z)-plan

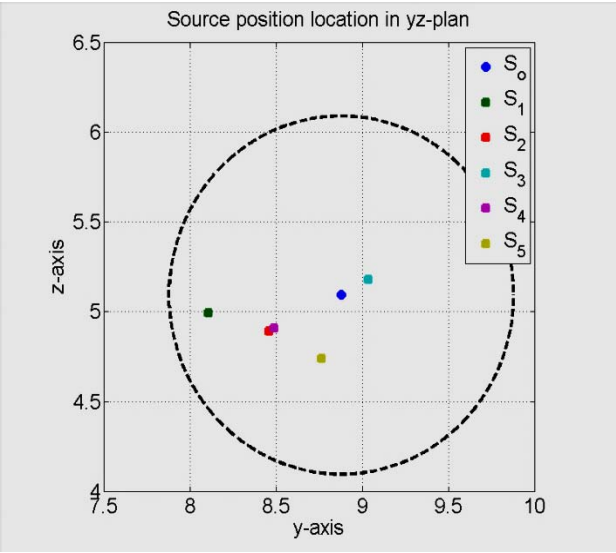

Fig. 10. Measured and actual sources observed in 2D (y , z)-plan

It can be seen that the placement 5 presents an accurate prediction followed respectively by placements 3, 4, 2 and 1 as shown in Fig. 8. The placements 1 and 5 into which the antennas are respectively perfectly horizontally and vertically aligned seem to be less accurate than the others when using the first peak method as compared to the cross correlation done by [1] with the same measurement data, where they were much accurate than the other placement. However placements 3 and 4 which are almost similar produced a measured source at almost the same distance from the actual source and that was indeed expected and that was also the case in the study of [1]. The errors as shown in Table X, as already discussed in [1] come mainly from the signal reflection due the placement of antennas quite close to each other. However these errors seemed not to influence the signal integrity and measurement, since they are quite small. Thus the arc source fault, when it occurs on the field, can immediately be discovered when this proposed algorithm is used. From the experiment and initial analysis, the outcomes are: (i) the conventional method of time difference, using the proposed signal first peaks´ arrival, works at a reasonable level of accuracy and (ii) the new proposed method of timing the first peak of the dominant signal shows its potential in clarifying the arrival time point. Also, clear is that we need more tests with longer distances of the antenna placement from the arc source in locations on random selection.

IV. Conclusion

This paper reported an experimental investigation of power arc source location using radio frequency measurements. The RF signal first peak arrival time method was applied to capture the signals' energy at each antenna to accurately determine the distance between the antenna and the actual power arcing source.

The investigation found that the method of first peak arrival time of signals, worked at a reasonable level of accuracy and that the proposed method of timing the first peak of the signal showed its potential in clarifying the location technique. Also, the investigation found that more tests were needed with longer distances of the antenna placement from the arc source in locations of random selection, before more conclusions can be made of the performance of the method in real field cases.

Acknowledgements

The authors gratefully acknowledge the contributions of Tatu Nieminen and Joni Klüss, for their work on building the laboratory experiment.

References

[1] Ble, F.Z., Lehtonen, M., Sihvola, A., Kim, C., Cross-correlation method for power arcing source monitoring system, (2014) *International Review of Electrical Engineering (IREE)*, 9 (2), pp. 440-452.

[2] Bartlett, E.J.; Moore, P.J.; *"Remote sensing of power system arcing faults"*, Advances in Power System Control, Operation and Management, 2000. APSCOM-00. 2000 International Conference on Vol. 1 , 2000, pp. 49–53.

[3] Moore, P.J.; Portugues, I.E.; Glover, I.A.; *"Radiometric location of partial discharge sources on energized high-Voltage plant"*, Power Delivery, IEEE Transactions on Vol. 20, 2005, pp. 2264-2272.

[4] Shihab, S.; Wong, K.L.; *"Detection of faulty components on power lines using radio frequency signatures and signal processing techniques"*, Power Engineering Society Winter Meeting, 2000. IEEE Vol. 4, 2000, pp. 2449–2452.

[5] Young, D.P.; Keller, C.M.; Bliss, D.W.; Forsythe, K.W.*; "Ultra-wideband (UWB) transmitter location using time difference of arrival (TDOA) techniques"*, Signals, Systems and Computers, 2003. Conference Record of the Thirty-Seventh Asilomar Conference on Vol. 2 , 2003, pp. 1225–1229.

[6] Sun, Y.; Stewart, B.G.; Kemp, I.J.*; "Alternative cross-correlation techniques for location estimation of PD from RF signal"*, Universities Power Engineering Conference, 2004. UPEC 2004. 39th International Vol. 1, 2004, pp. 143–148.

[7] ChyeHuat Peck; Moore, P.J.; *"A direction-finding technique for wide-band impulsive noise source"*, Electromagnetic Compatibility, IEEE Transactions on Vol. 43, 2001, pp. 149–1544.

[8] Yang, L.; Judd, M.D.; Bennoch, C.J.*; "Time delay estimation for UHF signals in PD location of transformers [power transformers]"*, Electrical Insulation and Dielectric Phenomena, 2004. CEIDP '04. 2004 Annual Report Conference, 2004, pp. 414-417.

[9] Azaria, M.; Hertz, D.; *"IEEE Transactions on Acoustics, Speech, and Signal Processing"*, Vol. 32, 1984, pp. 280-285.

[10] Soeta, Y.; Uetani, S.; Ando, Y.; *"Autocorrelation and cross-correlation analyses of alpha waves in relation to subjective preference of a flickering light"*, Engineering in Medicine and Biology Society, 2001. Proceedings of the 23rd Annual International Conference of the IEEE Vol. 1, 2001, pp. 635– 638.

[11] Alavi, B.; Pahlavan, K.; *"Modeling of the TOA-based distance measurement error using UWB indoor radio measurements"*, Communications Letters, IEEE Vol. 10, 2006, pp. 275–277.

[12] Mallat, Achraf; Louveaux, J.; Vandendorpe, L.; *"UWB based positioning: Cramer Rao bound for Angle of Arrival and comparison with Time of Arrival"*, 2006 Symposium on Communications and Vehicular Technology, pp. 65–68.

[13] Alsindi, N.; Xinrong Li; Pahlavan, K.; *"Analysis of Time of Arrival Estimation Using Wideband Measurements of Indoor Radio Propagations"*,Instrumentation and Measurement, IEEE Transactions on Vol. 56, 2007, pp. 1537-1545.

[14] Rohrig, C.,Kunemund, F., *"Mobile Robot Localization using WLAN Signal Strengths"*.Intelligent Data Acquisition and Advanced Computing Systems: Technology and Applications, 2007. IDAACS 2007. 4th IEEE Workshop, pp. 704 - 709

[15] Bo-ChiehLiu,Ken-Huang Lin *"Accuracy Improvement of SSSD Circular Positioning in Cellular Networks"*.Vehicular Technology, IEEE Transaction, pp. 1766 - 1774

[16] Motter, P. , Allgayer, R.S. ; Muller, I. ; Pereira, C.E. ; Pignaton de Freitas, E. *"Practical issues in Wireless Sensor Network localization systems using received signal strength indication"*.Sensors Applications Symposium (SAS), 2011 IEEE, pp. 227 - 232

[17] Chih-Chun Lin, She-Shang Xue; Yao, L. *"Position Calculating and Path Tracking of Three Dimensional Location System Based on Different Wave Velocities"*.Dependable, Autonomic and Secure Computing, 2009. DASC '09. Eighth IEEE International Conference, pp. 436 - 441

[18] El Arja, H., Huyart, B.; Begaud, X. *"Joint TOA/DOA measurements for UWB indoor propagation channel using MUSIC algorithm"*.Wireless Technology Conference, 2009, pp. 124 - 127

[19] Born, A.,Schwiede, M. ; Bill, R. *"On distance estimation based on radio propagation models and outlier detection for indoor localization in Wireless GeosensorNetworks"*,Indoor Positioning and Indoor Navigation (IPIN), International Conference 2010, pp. 1 - 6

[20] Fugen Su, WeizhengRen; Hongli Jin, *"Localization Algorithm Based on Difference Estimation for Wireless Sensor Networks"*.Communication Software and Networks. ICCSN '09. International Conference, 2009, pp. 499 - 503

[21] Bing-Fei Wu , Cheng-Lung Jen ; Kuei-Chung Chang, *"Neural fuzzy based indoor localization by Kalman filtering with propagation channel modeling"*. Systems, Man and Cybernetics. ISIC. IEEE International Conference, 2007, pp. 812 - 817

[22] Benkic, K., Malajner, M.; Planinsic, P.; Cucej, Z. *"Using RSSI value for distance estimation in wireless sensor networks based on ZigBee"*.Systems, Signals and Image Processing, 2008. 15th International Conference, 2008, pp. 303 - 306

[23] Suk-Un Yoon, Liang Cheng; Ghazanfari, E.; Pamukcu, S.; Suleiman, M.T. *"A Radio Propagation Model for Wireless Underground Sensor Networks"*.Global Telecommunications Conference (GLOBECOM 2011), 2011, pp. 1 – 5

Authors' information

Frank Zoko Ble obtained a B.Sc. in Physics in Ivory coast National University, Abidjan in 1997. He received M.Sc. in Electrical Engineering in Helsinki University of Technology (TKK), Espoo, Finland in 2010. He is a planning and design engineer for the City of Espoo, the central state-owned enterprise, Finland.Also, he is working toward his PhD degree in Aalto University, School of Electrical Engineering. His research interests are in electric power arcs detection using radio frequency measurements. He is a researcher in the Department of Electrical of Aalto University, School of Electrical Engineering, Finland.

Matti Lehtonen (1959) was with VTT Energy, Espoo, Finland from 19987 to 2003, and since 1999 has been a professor at the Helsinki University of Technology (TKK), where he is now head of Electrical Engineering department. Matti Lehtonen received both his Master's and Licentiate degrees in Electrical Engineering from Helsinki University of Technology , in 1984 and 1989 respectively, and the Doctor of Technology degree from Tampere University of technology in 1992. The main activities of Professor Lehtonen include power system planning and asset management, power system protection including earth fault problems, harmonic related issues and applications of information technology in distribution systems. He is a Professor in Aalto University, School of Electrical Engineering, Finland.

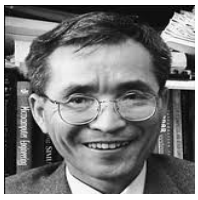

Charles Kim received a PhD degree in electrical engineering from Texas A&M University (College Station, TX) in 1989. Since 1999, he has been with the Department of Electrical and Computer Engineering at Howard University. Previously, Dr. Kim held teaching and research positions at Texas A&M University and the University of Suwon. Dr. Kim's research includes failure detection, anticipation, and system safety analysis in safety critical systems in energy, aerospace, and nuclear industries. Several inventions of his in the research area have been patent field through the university's intellectual property office. Dr. Kim is a senior member of IEEE and the chair of an IEEE chapter in Washington Baltimore section.

Ari Sihvola was born on October 6th, 1957, in Valkeala, Finland. He received the degrees of Diploma Engineer in 1981, Licentiate of Technology in 1984, and Doctor of Technology in 1987, all in Electrical Engineering, from the Helsinki University of Technology (TKK), Finland. Besides working for TKK and the Academy of Finland, he was visiting engineer in the Research Laboratory of Electronics of the Massachusetts Institute of

Technology, Cambridge, in 1985–1986, and in 1990–1991, he worked as a visiting scientist at the Pennsylvania State University, State College. In 1996, he was visiting scientist at the Lund University, Sweden, and for the academic year 2000–01 he was visiting professor at the Electromagnetic and Acoustics Laboratory of the Swiss Federal Institute of Technology, Lausanne. In the summer of 2008, he was visiting professor at the University of Paris XI, France. Ari Sihvola is professor of electromagnetic in Aalto University School of Electrical Engineering (former name before 2010: Helsinki University of Technology) with interest in electromagnetic theory, complex media, materials modeling, remote sensing, and radar applications. He is Chairman of the Finnish National Committee of URSI (International Union of Radio Science) and Fellow of IEEE. He also served as the Secretary of the 22nd European Microwave Conference, held in August 1992, in Espoo, Finland. He was awarded the ve-year Finnish Academy Professor position starting August 2005. He is also director of the Finnish Graduate School of Electronics, Telecommunications, and Automation (GETA).